

C. SENDEROWSKI*, Z. BOJAR*, W. WOŁCZYŃSKI**, G. ROY***, T. CZUJKO****

RESIDUAL STRESSES DETERMINED BY THE MODIFIED SACHS METHOD WITHIN A GAS DETONATION SPRAYED COATINGS OF THE Fe-Al INTERMETALLIC

NAPRĘŻENIA WŁASNE OKREŚLONE METODĄ SACHSA W POWŁOKACH NA BAZIE FAZ METALICZNYCH TYPU Fe-Al NANIESIONYCH METODĄ DETONACYJNĄ

A modified Sachs method was applied to determine the residual surface stress in Fe-Al type intermetallic coatings deposited on a surface of carbon 1045 steel substrate by a gas detonation spray technique. The detailed theoretical model with a description of device is presented. Compressive stresses in the entire thickness of created coatings is discussed. The influence of chemical composition of powders (applied for coating deposition) on residual stress related to the structural and phase composition, as well as the degree of chemical heterogeneity of the multilayer composite coating system is analyzed. The maximum amplitude of stress on the surface of coatings is within the range of -900 to -1100 MPa for samples without boron additive and between -500 and -600 MPa for samples with boron only. The composition of the powder blend of the FeAl-intermetallic coatings deposited on the surface of the substrate affects significantly the distribution of residual stresses. The structural inhomogeneity and no repeatability of physical and chemical properties of particular structural elements are the reasons for the development of residual stresses system generation within the coating.

Keywords: Residual stress, Gas Detonation Spraying, Intermetallic coatings, Sachs method

Zastosowano zmodyfikowaną metodę Sachsa, by określić stan rozkładu naprężeń własnych w głąb kolejnych warstw strukturalnych międzymetalicznych powłok typu Fe-Al, naniesionych metodą detonacyjną na stal węglową 45. Szczegółowo przedstawiono teoretyczny model obliczeniowy z opisem urządzenia pomiarowego. Stwierdzono obecność naprężeń ściskających w całej grubości badanych powłok. Analizowano wpływ składu chemicznego proszków (zastosowanych do otrzymania powłok) na naprężenia własne wielowarstwowego kompozytowego systemu powłokowego, określając właściwości strukturalne, skład fazowy, jak również stopień niejednorodności składu chemicznego powłok. Stwierdzono, że maksymalna wartość naprężeń własnych (-900 i -1100 MPa) występuje bezpośrednio w strefie przypoверхniowej powłok bez udziału boru i nieco mniejsze wartości z przedziału (-500 i -600 MPa) odnotowano dla powłok z dodatkiem boru. Wykazano, że skład chemiczny proszków użytych do natryskiwania detonacyjnego, wpływa na rozkład naprężeń własnych powłok międzymetalicznych typu Fe-Al natryskiwanych na podłożu stalowe. Stwierdzono, że również niejednorodność strukturalna, a w efekcie niepowtarzalność właściwości fizyko-chemicznych poszczególnych składników strukturalnych powłok, są bezpośrednią przyczyną generowania określonego układu naprężeń własnych w badanych powłokach.

1. Introduction

Iron aluminide intermetallic alloys are excellent candidates for application in medium to high temperature environments because of the combination of good mechanical properties, low density, low cost, availability of raw materials, remarkable resistance to erosion as well as sulfidizing and oxidizing at high temperature [1-4]. The major drawbacks of such alloys like low ductility and

brittleness at room temperature result in some difficulties in their shaping. To reduce these drawbacks microalloying additions of boron and zirconium and also reducing the grain size [5-7] is usually applied. It was indicated in some studies that Fe-Al intermetallic coatings on structural materials obtained by various methods can solve problems connected with a fabrication of these alloys into useful shapes as well as increase suitability for the effective use of their environment and wear resistance

* DEPARTMENT OF ADVANCED MATERIALS AND TECHNOLOGIES, MILITARY UNIVERSITY OF TECHNOLOGY, 00-908 WARSZAWA, 2 KALISKIEGO STR., POLAND

** INSTITUTE OF METALLURGY AND MATERIALS SCIENCE OF THE POLISH ACADEMY OF SCIENCES, 30-059 KRAKÓW, 25 REYMONTA STR., POLAND

*** NATURAL RESOURCES CANADA, CANMET/MTL, OTTAWA, ONTARIO, CANADA, K1A 0G1

**** DEPARTMENT OF MECHANICAL ENGINEERING, UNIVERSITY OF WATERLOO, WATERLOO, ONTARIO, CANADA N2L 3G1

[8-13]. Due to their high deposition rates and their relatively low cost, various thermal spray techniques were applied to produce thick iron aluminide deposits ranging from several tens of micrometers up to a few millimeters [8-12]. In this study, a promising processing technique, known as detonation gun spraying (DGS), is presented. The DGS method was developed and patented by Union Carbide in 1955, and developed independently in 1969 at the Institute of Materials Science, Kiev, Ukraine [14, 15]. The DGS process is realized by deposition of accelerated by the detonation wave particles and their impact on the substrate surface at a high velocity of 800-1200 m/s, which depends on the applied gas explosive mixture. Using this technique, one can produce a uniform and dense coating with high hardness and strong adhesion to the substrate, which shows good coating performance [15, 16].

The coating process in many cases leads to high intrinsic residual stresses within the coatings, which are known to have a significant influence on the mechanical properties, structure thermal stability, abrasive and erosive wear resistance, and corrosion resistance [17-19]. For this reason the analysis of the residual stress distribution with respect to the layer thickness by various methods has become increasingly important. Several different residual stress measurement techniques were briefly characterized by Totemeier et al. [18]. The techniques were roughly grouped into three categories: 1) measurement of crystallographic lattice parameters, 2) measurement of strain after layer removal or hole drilling, and 3) measurement of curvature of appropriately sized coating-substrate couples. The above techniques have intrinsic advantages and disadvantages.

In this paper, analysis of residual stress gradient with depth of DGS Fe-Al type coatings is performed by a modification of the well known Sachs method [20].

2. Materials and methods

2.1. Preparation of material and coatings

On the basis of the research carried out so far, the Fe-Al powders, with the composition presented in Table 1, and the average particle size in a range of 40-70 μm were selected for coating application by the gas detonation spray method. The powder was produced in the self-decomposition process and the system coating/substrate demonstrated the most advantageous geometric as well as physical and mechanical properties.

The gas detonation process of all coatings was carried out in the SAT (Surface Advance Technology) company in Warsaw with the optimum spraying parameters which influence detonation energy of the detonation

TABLE 1
Chemical composition and particle size of self-decomposed powders used for coating spraying

Sample	Alloying elements [at.%]					Powder particle size [μm]
	Fe	Al	B	C	Si	
1	49.25	48.25		1.5		40-71
2	47.45	46			6.55	40-71
3	53.4	45	0.1	1.5		40-63
4	58.4	40	0.1	1.5		40-63
5	58.5	40		1.5		40-63

blend directly influencing metallurgical quality of the coatings. The powder was heating at the temperature of 100°C for 15 mins directly before its deposition. The substrate was a 1045-steel plate hardened and tempered, ground, stress-relieved, cleaned in finally abrasive-blasted with 24 μm al-oxide, directly before spraying.

2.2. Characterization of structure

The structural and physical/chemical factors such as the change in the morphology and chemical composition of the individual grains as well as phase change susceptibility were analyzed, Table 2. The analysis of the influence of the chemical composition of applied powders on the structural and phase compositions, as well as the degree of chemical heterogeneity of the multilayer composite coating system was carried out by the use of Philips XL-30 scanning microscope integrated with DX4i – EDAX X-ray microanalysis.

2.3. Principle of the Sachs method

The residual stresses measurements in Fe-Al intermetallic coatings obtained by DGS technique were carried out with specially designed meter circuit based on the Sachs Method (SM), Fig.1. One side of the sample was mounted in a specimen holder (free-ends beam system) and then etched in an acid mixture (1:3 HNO_3 and HCl). In this meter system, indirect measure of level and direction of residual stresses in analyzed coating is calculated from the variation of the sample deflection line caused by removal of successive coatings in etching effect. All types of intermetallic layers were tested 3 times under identical conditions.

In the presented method, the effect of operations of system calibration on residual stresses measurement is eliminated. However, as a result of this, a very complex mathematical model is necessary. To carry out the calculations, MathCAD 5.0 software was applied.

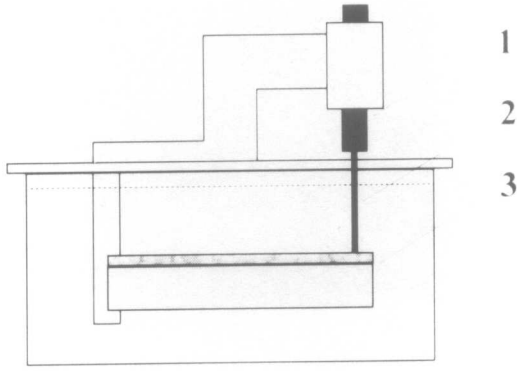


Fig. 1. A schematic drawing of equipment to measure deflection of the plate. 1 – displacement sensor, 2 – push rod, 3 – sample (in the coating/substrate system)

2.4. Formulation of mathematical model and its modification

Residual stress analysis by the Sachs method consists in evaluating residual stress distribution $\sigma(h)$ as a function of distance from surface as a difference:

$$\sigma(h) = \sigma_p(h) - \sigma_d(h) \quad (1)$$

where $\sigma_p(h)$ – residual stress existing in the surface layer at a depth of h , after removing previous layers; $\sigma_d(h)$ – additional residual stresses arising in analyzed layer as a result of successive removal of the previous layer.

To determine residual stress variation with depth, $\sigma(h)$, a bending moment dM , equivalent to the moment of average stress existing in the layer to be removed, is applied. If the removed layer is infinitesimal of (differential) thickness dh , the bending moment dM is given by:

$$dM = \frac{1}{2} \sigma_p(h) b (h_0 - h) dh \quad (2)$$

For a beam with a free-end, the bending moment can also be expressed as

$$dM = \frac{8EJ}{L^2} df \quad (3)$$

where f is the vertical deflection at the end of the plate, see Fig. 2, which is also related to the change in the curvature of the plate. Therefore, the geometrical location of the centre of curvature varies during layer removal. Equating right sides of Equations (2) and (3) and solving for $\sigma_p(h)$ results in

$$\sigma_p(h) = \frac{4E(h_0 - h)^2}{3L^2} \frac{df}{dh} \quad (4)$$

where h_0 – sample thickness before successive layer removal; b – sample width with DGS coating; $E = 2.1 \cdot 10^5$

[MPa] – Young's modulus of target material; J [m⁴] – moment of inertia of sample section in respect of the neutral axis; L [m] – the distance between extreme layers of sample section and neutral axis.

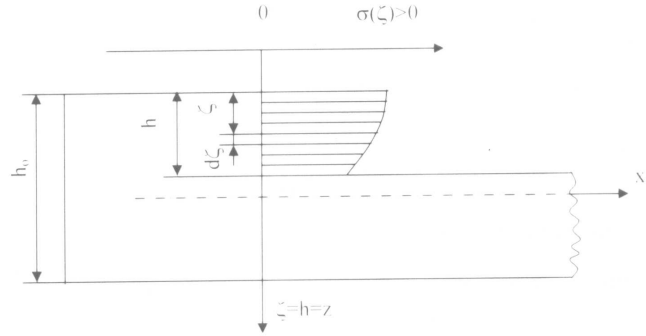


Fig. 2. A cross-section of the plate with imaginary differential layers and the variables applied to residual stress analysis

To determinate simultaneously $\sigma_p(h)$ as well as $\sigma_d(h)$, the auxiliary variable ζ , Fig. 2, [20] is introduced. Hence Equation (4) can be rewritten as:

$$\sigma_p(h) = \frac{4E(h_0 - \zeta)^2}{3L^2} \frac{df}{dh} \quad (5)$$

The additional stresses, arising as an effect of removal of successive layers, are determined by using the force normal to the section and equivalent moment of force:

$$\sigma_d(h) = \frac{4E}{3L^2} \left[4(h_0 - h) f(h) - 2 \int_0^h f(\zeta) d\zeta \right] \quad (6)$$

Introducing formulas {5} and {6} into Equation {1}, it yields:

$$\sigma(h) = \frac{4E}{3L^2} \left[(h_0 - h)^2 \frac{df}{dh}(h) - 4(h_0 - h) f(h) + 2 \int_0^h f(\zeta) \right] \quad (7)$$

Thus, after several mathematical transformations, residual stress $\sigma(h)$ can be determined as:

$$\sigma(h) = M [A(h) + B(h) + C(h)] \quad (8)$$

where: $M = \frac{4E}{3L^2}$ is a constant dependent on material, sample geometry and applied design (which in the considered case is a free-end beam system); $A(h) = (h_0 - h)^2 \frac{df}{dh}(h)$ is the term dependent on the derivative;

and $C(h) = 2 \int_0^h f(\zeta) .d\zeta$ is the term dependent on the integral in Equation {7}.

Determining the ranges of h corresponding to the thicknesses of layers at depths $h_0, h_1, h_2, \dots, h_n$ as well as connected with them the values of deflection, Fig. 3, [20-22], it is possible to determine the derivative $\frac{df}{dh}(h_i)$ numerically (applying the Lagrange interpolation polynomial):

$$\begin{aligned} \frac{df}{dh}(h) \approx & f_{i-1} \frac{2h - h_i - h_{i-1}}{(h_{i-1} - h_i)(h_{i-1} - h_{i+1})} + \\ & + f_i \frac{2h - h_{i-1} - h_{i+1}}{(h_i - h_{i-1})(h_i - h_{i+1})} + \\ & + f_{i+1} \frac{2h - h_{i-1} - h_i}{(h_{i+1} - h_{i-1})(h_{i+1} - h_i)} \end{aligned} \quad (9)$$

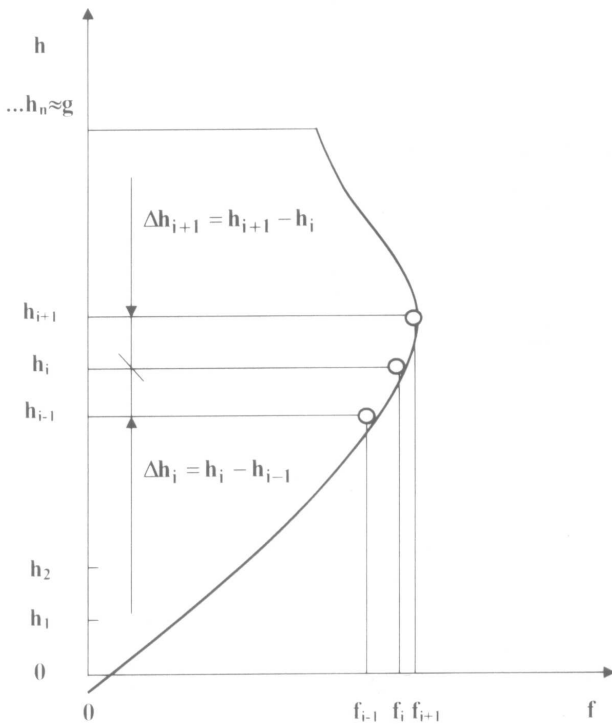


Fig. 3. Variation of deflection f with the depth below the surface of coating

Taking into account the thicknesses of successively removed layers described as:

$$\left. \begin{aligned} \Delta h_i &= h_i - h_{i-1} \\ \Delta h_{i+1} &= h_{i+1} - h_i \end{aligned} \right\} \quad (10)$$

Equation {9} can be transformed into:

$$\begin{aligned} \frac{df}{dh}(h_i) = & f_{i-1} \left[\frac{-\Delta h_{i+1}}{\Delta h_i (\Delta h_i + \Delta h_{i+1})} \right] + \\ & + f_i \left[\frac{\Delta h_{i+1} - \Delta h_i}{\Delta h_i \Delta h_{i+1}} \right] + f_{i+1} \left[\frac{\Delta h_i}{\Delta h_{i+1} (\Delta h_i + \Delta h_{i+1})} \right] \end{aligned} \quad (11)$$

or:

$$\frac{df}{dh}(h_i) = f_{i-1} K_i + f_i L_i + f_{i+1} M_i, \quad (11a)$$

where $K_i, L_i,$ and M_i denote the right multipliers of the respective terms in Equation {11}. If the boundary conditions are applied, it yields:

for $i = 0$

$$\begin{aligned} \frac{df}{dh}(h_0) = & f_1 \frac{\Delta h_1 + \Delta h_2}{\Delta h_1 \Delta h_2} + \\ & + f_2 \left[\frac{-\Delta h_1}{\Delta h_2 (\Delta h_1 + \Delta h_2)} = f_1 L_0 + f_2 M_0 \right], \quad \text{and} \end{aligned} \quad (12)$$

for $i = n$

$$\begin{aligned} \frac{df}{dh}(h_n) = & f_{n-2} \left[\frac{\Delta h_n}{\Delta h_{n-1} (\Delta h_{n-1} + \Delta h_n)} \right] + \\ & + f_{n-1} \left[\frac{-(\Delta h_{n-1} + \Delta h_n)}{\Delta h_{n-1} \Delta h_n} \right] + \\ & + f_n \left[\frac{\Delta h_n + (\Delta h_{n-1} + \Delta h_n)}{\Delta h_n (\Delta h_{n-1} + \Delta h_n)} \right] = f_{n-1} K_n + f_{n-1} L_n + f_n M_n \end{aligned} \quad (12a)$$

The integral in Equation {7} can be approximated numerically:

$$\int_0^h f(\zeta) d\zeta \approx \sum_{u=0}^{u=i} \frac{\Delta h_u}{2} (f_{u-1} + f_u) \quad (13)$$

Applying:

$$\frac{df}{dh}(h) \approx \frac{f(h)}{h}$$

Equation {12} takes the form:

$$\int_0^h f(\zeta) d\zeta = \frac{1}{2} f(h) h \quad (14)$$

Hence the variation of residual stress described by Equation {7} can be represented by:

$$\sigma(h) = \frac{4E}{3L^2} \left[(h_0 - h) \frac{f(h)}{h} - 4(h_0 - h) f(h) + f(h) h \right] \quad (15)$$

The accuracy of residual stress measurements was estimated as a sum of two terms:

$$\bar{\sigma} = \sigma \pm \Delta\sigma \quad (16)$$

$$\Delta\sigma = \begin{cases} \frac{R(\sigma)}{2} = \frac{\sigma_{\max} - \sigma_{\min}}{2} \\ \frac{t_{\alpha}}{\sqrt{r}} S(\sigma) \end{cases}$$

where: r – number of measurements corresponding to the number of samples;

t_{α} – confidence coefficient for the t-student distribution;

$R(\sigma)$ – range of residual stresses;

$\sigma_{\max}, \sigma_{\min}$ – principal or maximum and minimum components of residual stress states at different depths;

$S(\sigma)$ – standard deviation corresponding to stress Φ ,

$$S(\sigma) = \sqrt{\frac{1}{r-1} \sum_{i=1}^r (\sigma_i - \sigma)^2} \quad (17)$$

where for the confidence coefficient $\alpha = 0.05$, the number of tests $r = 3$, and the confidence coefficient for the t-student distribution is $t_{\alpha} = 4.302$.

2.5. Residual stress determination

The magnitude of average residual stresses and their standard deviations in corresponding layers of each coating was performed applying Equations (11a) and (16). The deflection listed in Table 3 recorded after removal of successive layers in one of kind each coating for example. The resultant (calculated) stress variations in investigated areas of layers are listed in Table 4 (example for the first test applied to a given coating). The variations are presented graphically in Fig. (5) and Fig. (6).

TABLE 2
Chemical composition in selected areas of coating 2, Fig. (4b)

Analyzed area	Composition (at. %)		
	Fe	Al	O ₂
“Gray” – FeAl	43.5	50.1	6.4
“Brightest” – Fe ₃ Al	64.2	25.2	10.7
“Dark gray” – FeAl ₂	25.8	53.4	20.8

TABLE 3
Variation of deflection after successive removal of layers (example for 1st test)

Layer	Deflection [mm]				
	Coating #				
	1	2	3	4	5
1	0.069	0.036	0.153	0.258	0.037
2	0.078	0.057	0.189	0.285	0.074
3	0.088	0.091	0.233	0.329	0.150
4	0.107	0.114	0.280	0.378	0.169
5	0.126	0.126	0.292	0.388	0.210
6	0.173	0.194	0.324	0.420	0.313
7	0.363	–	–	–	–

TABLE 4
Variation of residual stress in layers of five coatings (example for 1st test)

Layer	Stress [MPa]				
	Coating #				
	1	2	3	4	5
0	–1083	–951	–488	–561	–827
1	–941	–595	–396	–430	–323
2	–911	–559	–361	–364	–273
3	–669	–458	–266	–191	–107
4	–415	–384	–228	–187	–47
5	–322	–292	–213	–184	–50
6	–131	–99	–179	–123	–24
7	+259	–	–	–	–

3. Analysis of results and discussion

3.1. Structural characterization

Under conditions of identical DGS processes and the same substrate pre-processing, the fabricated FeAl coatings showed practically identical structure, morphology, distribution of phases and the structure of the coating/substrate bond, Fig. (4), regardless of the chemical composition of the powder blend sprayed, Table 1. A microstructure typical for the DGS method comprising the layered and flattened grains of the intermetallic phases from the Fe-Al system with the predominant FeAl phase (depicted by the grey area in the BSE pictures, Fig.(4b) was observed. The varying chemical composition of the microstructure, determined according to the equilibrium system of the compositional range of the existence of the FeAl intermetallic, ranges from 35 to 50%at. Al. On the basis of the point EDS analysis, Table 2, the low-aluminum Fe₃Al (which are the brightest areas in Fig. (4b) and the FeAl₂ phases (which are dark grey in Fig. (4b) were also identified. The observed grains of

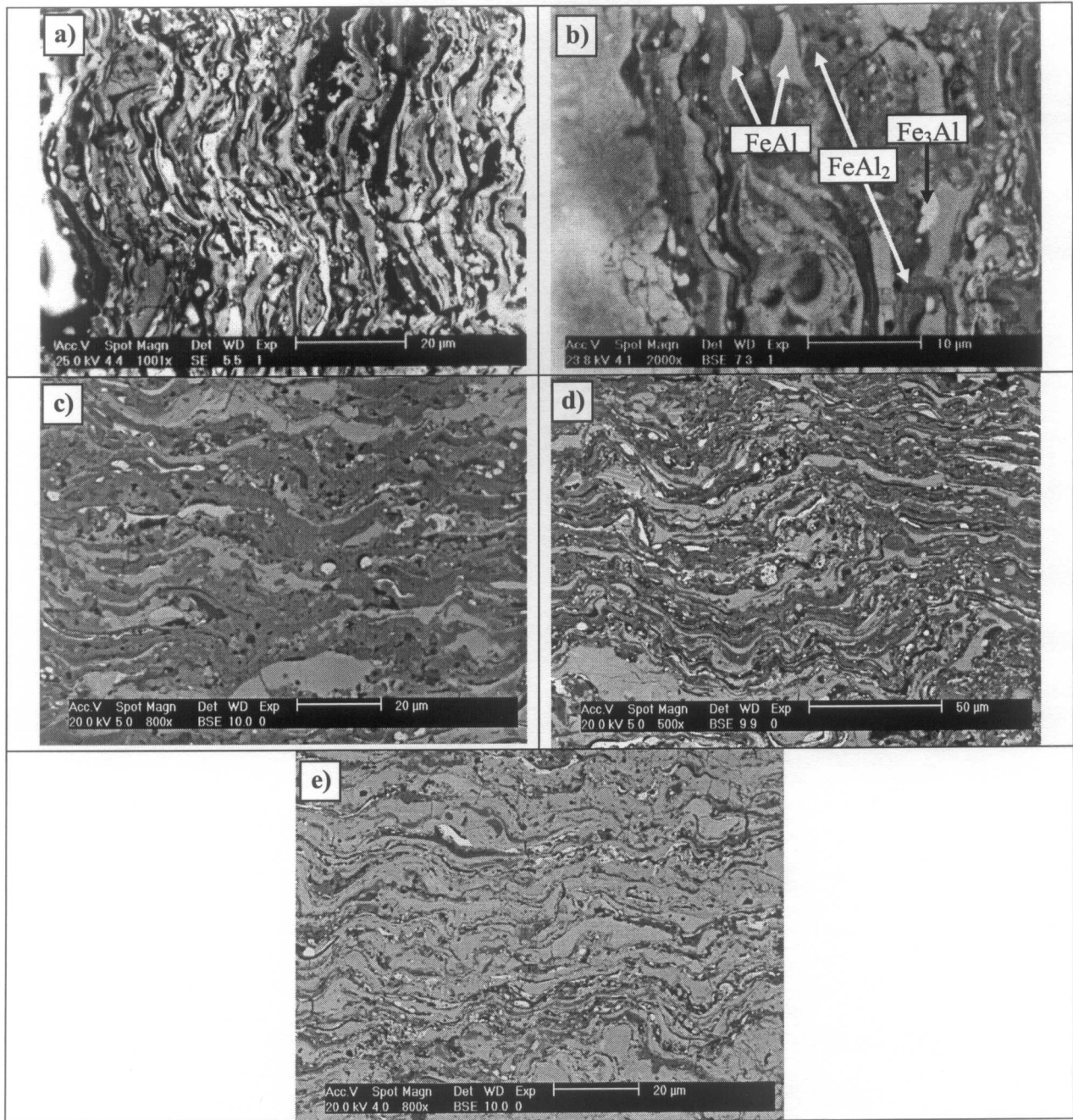


Fig. 4. Typical back-scattered SEM micrographs of coatings; cross-sections obtained from coating c1, a) coating c2, b), coating c3, c), coating c4, d), and coating c5, e)

the phases from the Fe-Al system correspond directly to the particles of intermetallic phases pre-existing in the powder mixture used for spraying.

They become ductile during the DGS process, although they show high degree of brittleness while subjected to unconstrained deformation, and convert into the flattened grains although they do not exhibit any traces of partial melting. This probably resulted in the reten-

tion of the phase structure and chemical composition. The aluminum-rich Fe-Al powder is chemically active in the DGS process such that all powder particles are already oxidized and the obtained coatings always contain oxide films inside the coating and at the residual interfaces. It is the formation of the oxide films (which are the darkest areas of the coating structure in Fig. (4)), which brings about the composite character of the Fe-Al

coatings. This observation is of great technological importance as the results obtained prove that, in the DGS conditions, the increased formation of Al_2O_3 protective scales on the surface of grains does not result in the segregation of impurities or microelements to the grain boundaries and therefore effectively protects the coatings against hydrogen diffusion which causes hydrogen embrittlement (which is very dangerous for Fe-Al intermetallic alloys in the temperature of the environment) and against inner oxidation and the influence of aggressive environment in the elevated temperature.

However, it must be remembered that both the inhomogeneity of the structure (and as the result the uniqueness of the physic-chemical features of the structural component of the coatings and especially the coefficient of heat expansion) as well as considerable non-dilatational strain resulting from the DGS process are direct cause of generating internal stresses in the coating and in the coating/substrate joint.

Therefore during the analysis of the internal strain in the DGS coatings one has to bear in mind both the influence of the dynamics of changes of the conditions of the DGS process (cyclic changes of the temperature and pressure – controlled by the spraying parameters) as the sequential character of formation of inhomogeneous coating (grain after grain, layer after layer) The research of the distribution of internal strain distribution in the D-gun sprayed coatings according to the Sachs method allow for unambiguous definition of the character and quantity of strain in the subsequent structural layers of the gas detonation coatings.

3.2. Residual stress analysis

The residual stress distribution in consecutive structural layers, Figs. (5-6), shows that in the tested coatings compressive stresses are observed. Their maximum value is on the surface of the coatings, what can strongly affect the coatings' functional quality. Generally, in all types of the tested coatings, similar characteristic changes of residual stresses as a function of distance from surface were observed. The maximum values observed on the surface of the coatings are between -900 and -1100 MPa for the samples without boron additive, (c1, c2, c5), and between -500 and -600 MPa for samples with boron, (c3 and c4). The advantages of the current FeAl coatings is evident if comparison of residual stresses in FeAl coatings is made by the high-velocity oxy-fuel (HVOF) technique, where the compressive stresses can be in a range of -10 and -30 MPa and only up to -180 and -200 MPa [10]. The FeAl coatings obtained by DGS method in the studied cases can be characterized by compressive residual stresses which are 100 times greater than the stresses in coatings

made by HVOF technique. The residual stresses vary monotonically from their algebraically minimum (negative) magnitudes to -100 for coatings c2, c3, c4 and c5, and to higher up 200MPa for coating c1. In effect, the 0-stress axis (i.e. the axis of sign change) of the coating/substrate system is located for coatings c1 and c5 near the interface of the coating/substrate plates. This effect is particularly obvious for coating c1, where at the interface layer tensile stresses are observed, whereas the stress distribution in coatings c2, c3 and c4 still increases algebraically below the interface (within 150 μm) in the substrate towards the zero-stress magnitude, not reaching it though at all. The advantageous compressive stresses in the intermetallic DGS layers are mainly the result of overlapping various physical and chemical effects, which are typical for gas spraying of aluminum rich coatings. The aluminum rich intermetallic phases, can be characterized by high chemical affinity to oxygen, brittleness and the possibility of strengthening by plastic deformation as well as in the effect of vacancy freezing.

Essentially, thermal expansion of Al-rich intermetallic phases is much greater than thermal expansion of constructional steel, what should generate the tension stresses in cooled-down coatings. However, after the DGS process, the (unequivocal) presence of residual compressive stresses in the coatings was observed. This can be an effect of specific conditions during gas detonation spraying, such as high kinetic energy resulting in hydrodynamic plastic deformation of slightly softened particles, weak thermal interaction and complex phase structure of formed coating with a participation of oxide particles and films, which block deformation and make it difficult for grains to change size with temperature changes. This stress system in the investigated coatings essentially can be distinguished from a typical tensile stress system, which appears in another type of gas thermal coatings. The coatings obtained by gas detonation spraying method has a form of small powder particles situated on the substrate, which is created by the metallic spray stream.

The joint between the sprayed powder and the substrate as well as following layers is a result of kinetic energy and heat cumulated in a diphasic metallic spray stream, which consists of sprayed powder particles and products of detonation. As a result of strike of powder particles onto substrate material, the local temperature of the substrate increases and the so-called operating zone is observed. The intensity of local substrate heating depends on powder particles temperature, temperature of detonation products as well as temperature increase related to deformation of sprayed powder particles resulting from their strike onto substrate. Nevertheless, through an optimal selection of technological parameters (individual

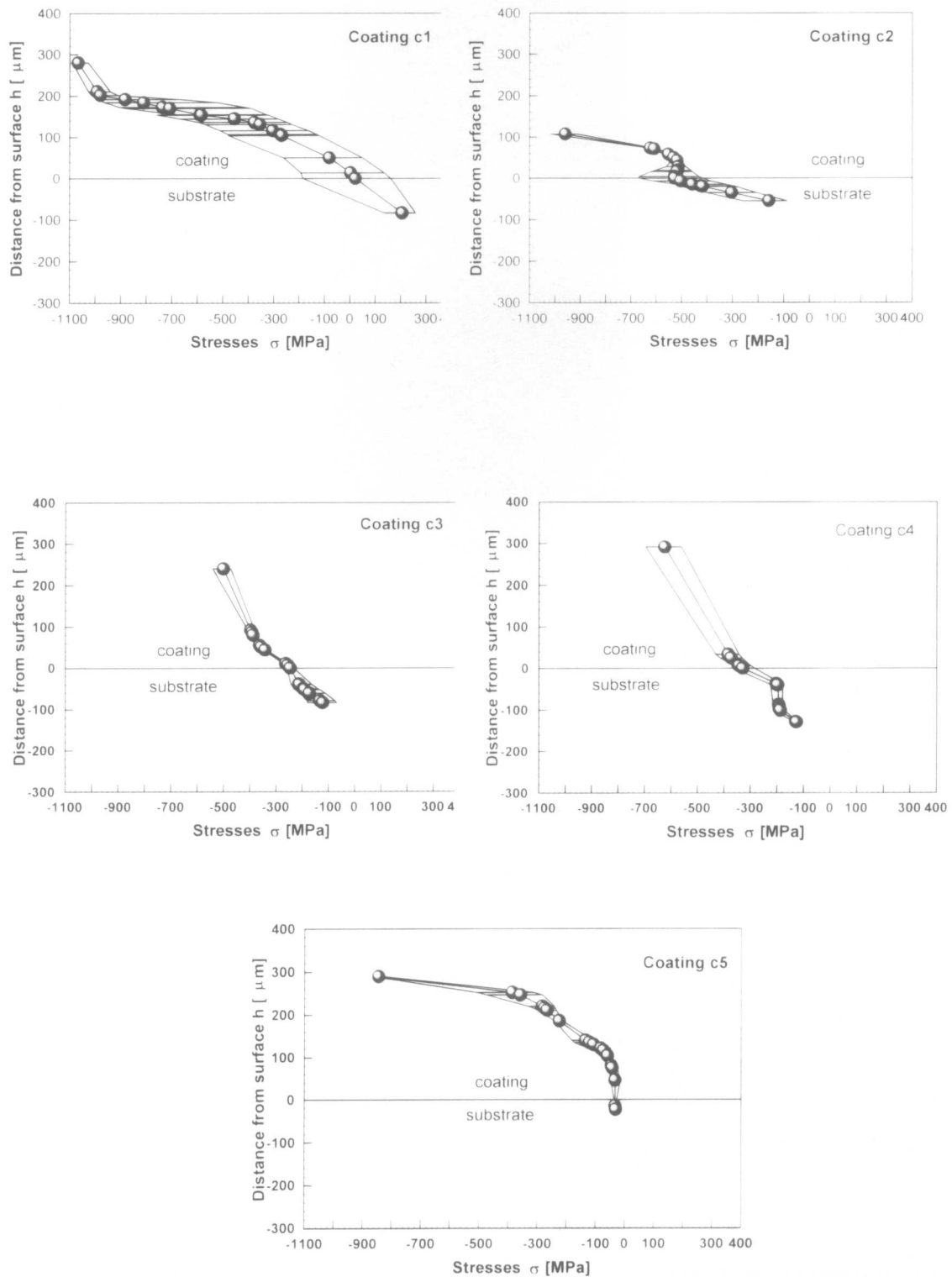


Fig. 5. Residual stress distributions above and below the coating/substrate interface for FeAl coating

for every coating material) the substrate material temperature increases slightly and it never exceeds 100°C. The kinetic energy of powder particles depends on the kind, size and shape of particles as well as the speed

of detonation products, which can be controlled by a proper selection of technological parameters. As a result of an enormous kinetic energy of diphase metallic spray stream, the particles of powder strike the substrate and

strengthen it by plastic deformation. Elastic and plastic strains involved in the system result in an increase of defect concentration, local atomic lattice structure destruction and formation of residual stresses in the surface layer of the substrate material.

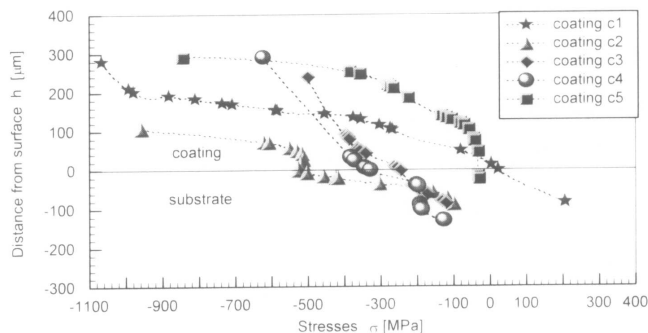


Fig. 6. A collective chart of residual stress distributions in the FeAl-coatings

The changes of mechanical properties of the substrate material depend on many factors, such as: shape, size, hardness, density, glancing angle or speed powder particles as well as the mechanical properties of substrate raw material.

Generally, for metals, after the gas detonation spray process, around 20% strengthening in surface layer compared to the substrate material is observed. The strengthening depth depends on type of substrate material, surface layer preparation before DGS process, sprayed powder properties and technological parameters.

4. Conclusions

1) The composition of the powder blend FeAl – intermetallic coatings deposited on the surface of the quenched and tempered 1045 - steel substrate through gas detonation spraying affects the distribution of residual stress.

2) Compressive residual stresses appear in almost all five types of coatings.

3) The maximum values of stress observed on the surface of coatings are around –900 and –1100 MPa for samples without boron additive and between –500 and –600 MPa for samples with boron. The values of residual stresses decrease monotonically from their minimum to 0 for coatings c2, c3, c4 and c5 and to higher up 200 MPa for coating c1.

4) In the case of gas thermal coatings, the type of selected method exerts significant influence on the residual stress distribution. In analysis of residual stresses in gas detonation sprayed coatings, the influence of dynamics changing of process conditions (temperature and pres-

sure) and sequent character of layer formation process must be taken into consideration.

5) The structural inhomogeneity and no repeatability of physical and chemical properties of particular structural elements are the reasons for the development of residual stresses system generation in the coating and on the bonding coating/substrate.

Acknowledgements

The authors express their thanks Prof. W. Przetakiewicz from the Military University of Technology, Warsaw, Poland for the helpful discussions. The work is supported by the Polish Committee for Scientific Research, grant No 0026/T02/2006/30.

REFERENCES

- [1] C. G. Mc Kamey, J. H. De Van, P. E. Tortorelli, V. K. Sikka, *Journal of Material Research* **6**, 8, 1779 (1991).
- [2] Y. Yang, I. Baker, *Intermetallics* **6**, 167 (1998).
- [3] Cebulski, S. Lalik, R. Michalik, *Advanced Materials & Technologies 'AMT 2007' Inżynieria Materiałowa 3-4*, 757 (2007).
- [4] C. Senderowski, Z. Bojar, W. Przetakiewicz, *Archives of Foundry Engineering* **7**, 1/2007, 147 (2007).
- [5] D. G. Morris, S. Gunter, *Materials Science and Engineering* **A208**, 7 (1996).
- [6] S. C. Deevi, V. K. Sikka, C. T. Liu, *Progress in Material Science* **42**, 177 (1997).
- [7] A. S. Gay, A. Frączkiewicz, *Journal de Physique IV, Colloque 2, Supplement au Journal de Physique III* **6**, 223 (1996).
- [8] B. Xu, Z. Zhu, S. Ma, W. Zhang, W. Liu, *Wear* **257**, 1089 (2004).
- [9] T. Grosdidier, A. Tidu, H-L. Liao, *Scripta Materialia* **44**, 387 (2001).
- [10] T. C. Totemeier, R. N. Wright, W. D. Swank, *Intermetallics* **12**, 1335 (2004).
- [11] S. Pal Dey, S. C. Deevi, *Material Science and Engineering* **A355**, 208 (2003).
- [12] G. Ji, T. Grosdidier, H-L. Liao, J.-P. Morniroli, C. Coddet, *Intermetallics* **13**, 596 (2005).
- [13] Z. Bojar, C. Senderowski, T. Czujko, R. A. Varin, *Proc. of 13th Canadian Materials Science Conference, Sudbury, Ontario*, 23 (2001).
- [14] E. Kadyrov, V. Kadyrov, *Adv. Mater. Process.* **8**, 21 (1995).
- [15] P. L. Ke, Y. N. Wu, Q. M. Wang, J. Gong, C. Sun, L. S. Wen, *Surface & Coating Technology* **200**, 2271 (2005).
- [16] C. Senderowski, Z. Bojar, *Int. J. App. Mech. and Eng.* **9**, 65 (2004).

- [17] Ch. Genzel, W. Reimers, *Surface & Coating Technology* **116-119**, 404 (1999).
- [18] T. C. Totemeier, K. J. Wright, *Surface & Coating Technology* **200**, 3955 (2006).
- [19] J. Wang, P. Shrotriya, K.-S. Kim, *Experimental Mechanics* **46**, 39 (2006).
- [20] Von G. Sachs, Der Nachweis innerer Spannungen in Stangen und Rohren, *Zeitschrift für Metallkunde*, 19 Jahrgang, 9, 352 (1927).
- [21] M. Mesnager, Methode de determination des tensions existant dans un cylindre circulaire, *Comptes Rendus, Hebdomadaires, Des Sciences de l'Academie des Sciences*, Tome 169, Juillet - Decembre, Seance du 29 Decembre: p.1391 (1919).
- [22] D. Rosenthal, J. T. Norton, *The Welding Journal* **24**, 295 (1945).

Received: 20 May 2007.